



Contents lists available at ScienceDirect

Molecular and Cellular Endocrinology

journal homepage: www.elsevier.com/locate/mce

Extramitochondrial OPA1 and adrenocortical function

Q1 László Fülöp^a, Anikó Rajki^b, Dávid Katona^a, Gergő Szanda^a, András Spät^{a,*}^a Department of Physiology, Faculty of Medicine, Semmelweis University, Hungary^b Laboratory of Molecular Physiology, Hungarian Academy of Sciences, POB 259, H-1444 Budapest, Hungary

ARTICLE INFO

Article history:

Received 10 June 2013

Received in revised form 19 July 2013

Accepted 19 July 2013

Available online xxxxx

Keywords:

Optic Atrophy 1

Aldosterone

Perilipin

Hormone sensitive lipase

Mitochondria

H295R cell

ABSTRACT

We have previously described that silencing of the mitochondrial protein OPA1 enhances mitochondrial Ca^{2+} signaling and aldosterone production in H295R adrenocortical cells. Since extramitochondrial OPA1 (emOPA1) was reported to facilitate cAMP-induced lipolysis, we hypothesized that emOPA1, via the enhanced hydrolysis of cholesterol esters, augments aldosterone production in H295R cells. A few OPA1 immunopositive spots were detected in ~40% of the cells. In cell fractionation studies OPA1/COX IV (mitochondrial marker) ratio in the post-mitochondrial fractions was an order of magnitude higher than that in the mitochondrial fraction. The ratio of long to short OPA1 isoforms was lower in post-mitochondrial than in mitochondrial fractions. Knockdown of OPA1 failed to reduce db-cAMP-induced phosphorylation of hormone-sensitive lipase (HSL), Ca^{2+} signaling and aldosterone secretion. In conclusion, OPA1 could be detected in the post-mitochondrial fractions, nevertheless, OPA1 did not interfere with the cAMP – PKA – HSL mediated activation of aldosterone secretion.

© 2013 Published by Elsevier Ireland Ltd.

1. Introduction

The precursor of corticosteroids is cholesterol. Cholesterol may be synthesized within the endoplasmic reticulum or taken up from plasma lipoproteins. Cholesterol esters, taken up by endocytosis of receptor-bound LDL particles, are hydrolyzed in the endoplasmic reticulum. More important for steroid biosynthesis is HDL-transported esterified cholesterol, taken up by scavenger receptor B1 (Rone et al., 2009) and hydrolyzed by cholesterol esterase (Rodríguez et al., 1999). The esterase was recently found to be identical with the HSL of lipocytes (Kraemer et al., 2004). Following reesterification cholesterol accumulates in special, phospholipid layer bounded droplets. Rapid increase of cortisol secretion during stress or increased aldosterone secretion during acute fluid loss requires the rapid mobilization of cholesterol stored in these lipid droplets (Hattangady et al., 2011; Vinson et al., 1992). Deesterification is performed again by HSL (Kraemer et al., 2004).

Abbreviations: $[\text{Ca}^{2+}]_m$, mitochondrial Ca^{2+} concentration; AKAP, A-kinase anchoring protein; CaMKII, Ca^{2+} /calmodulin-dependent kinase II; COX IV, cytochrome c oxidase IV; db-cAMP, dibutyl- cAMP ; emOPA1, extramitochondrial OPA1; HSL, hormone-sensitive lipase; IMM, inner mitochondrial membrane; IMS, mitochondrial intermembrane space; Mfn 1, mitofusin 1; OMM, outer mitochondrial membrane; OPA1, Optic Atrophy 1; PDI, protein disulfide isomerase; PKA, protein kinase A; Plin, perilipin; StAR, Steroidogenic Acute Regulating Protein; TSPO, (mitochondrial) Translocator Protein (previously peripheral benzodiazepine receptor).

* Corresponding author. Tel.: +36 1 4591500; fax: +36 1 2667480.

E-mail address: spat@eok.sote.hu (A. Spät).

The dual action of HSL is under hormonal control. ACTH, through cAMP-PKA, phosphorylates and thus activates the enzyme (Hirsch and Rosen, 1984; Holm et al., 2000; Kraemer et al., 2004; Trzeciak and Boyd, 1974) and also induces its expression (Granneman and Moore, 2008; Holysz et al., 2011). Calcium ion, the second messenger of angiotensin II, acts via CaMKII to activate (Cherradi et al., 1998) and through p42/p44 mitogen-activated protein kinase (Cherradi et al., 2003) to increase the expression of HSL.

Transfer of the released cholesterol to the side-chain cleaving enzyme cytochrome P450_{sc} (CYP11A1), located in the IMM, is carried out by a complex of cytosolic and mitochondrial proteins (Rone et al., 2009). At least two components of this complex, StAR and the translocator protein TSPO (previously named as peripheral benzodiazepine receptor) are phosphorylated and induced by PKA (Dyson et al., 2008; Fleury et al., 2004; Manna et al., 2002; Midzak et al., 2011). Although Ca^{2+} - mobilizing agonists (through Ca^{2+} and protein kinase C) were also reported to phosphorylate StAR (Betancourt-Calle et al., 2001; Cherradi et al., 1998) their major effect is the induction of StAR expression (Clark et al., 1995; Lucki et al., 2012; Martin et al., 2008).

In adipocytes activated PKA phosphorylates and brings about translocation of the cytosolic HSL to the membrane fraction (Hirsch and Rosen, 1984). This translocation requires the 62-kDa protein perilipin 1 (Plin 1) located on the surface of lipid droplets (Greenberg et al., 1991; Miyoshi et al., 2006). It is assumed that non-phosphorylated Plin 1 inhibits the access of phosphorylated HSL to its substrate (Brasaemle et al., 2009; Sztalryd et al., 2003; Tansey

et al., 2001; Zhang et al., 2003). Albeit PKA-mediated phosphorylation of Plin is not required for the translocation, phosphorylation is essential for hormone-induced lipolysis (Miyoshi et al., 2006). It is assumed that phosphorylation of Plin 1 permits the activation of adipocyte triglyceride lipase (Granneman et al., 2011; Subramanian et al., 2004; Yamaguchi et al., 2007) which provides diacylglycerol for further hydrolysis by HSL (Zimmermann et al., 2004).

A recently described factor participating in hormonally-induced lipolysis is Optic Atrophy 1 (OPA1). OPA1 (and its ortholog Mgm1p in yeast) has been known as a dynamin-related mitochondrial GTPase protein. In cooperation with Mitofusin 1 (Mfn 1) OPA1 induces mitochondrial fusion and its mutation is the most common cause of type 1 autosomal dominant optic atrophy (Belenguer and Pellegrini, 2012; Cipolat et al., 2004). Unexpectedly, OPA1 has been detected in lipocytes on the surface of Plin-coated lipid droplets (Pidoux et al., 2011). Immunocytochemical and immunoprecipitation studies showed that PKA binds to the Plin-associated OPA1 and the formation of this complex results in Plin phosphorylation and lipolysis. OPA1 contains an A-kinase binding domain and thus it may function as an AKAP. In fractionation studies the amount of OPA1 in the lipid droplet fraction far exceeded that in the mitochondrial fraction. Based on these observations a significant role has been attributed to OPA1 in the hormonal control of lipolysis, assuming that OPA1 potentiates the phosphorylation of Plin 1 by PKA and thus makes further steps possible (presumably the activation of adipocyte triglyceride lipase) (Greenberg et al., 2011; Pidoux et al., 2011). We are not aware of studies on emOPA1 in cell types other than adipocyte.

In humans OPA1 has eight mRNA isoforms and the expressed proteins can be separated in five bands between 96 and 84 kDa in Western blots. The two higher-molecular mass bands, the so-called long isoforms are mixture of isoforms 1, 2, 4 and 7 whereas the three short isoforms contain proteolytic products of the long ones and also isoforms 3, 5, 6 and 8. The long isoforms are attached to the IMM, the soluble short ones were found in the IMS partly associated to the OMM (Delettre et al., 2000; Lenaers et al., 2009; Liesa et al., 2009). OPA1 controls the diameter of the junction of cristae (Scorrano et al., 2002) and thus modifies the molecular diffusion between the lumen of the cristae and the IMS (Frey et al., 2002) and/or between the boundary (inner) and crista membrane (Sukhorukov and Bereiter-Hahn, 2009). Knockdown of OPA1 in

H295R human adrenocortical cells, probably due to the altered diffusion conditions, facilitates the transfer of cytosolic Ca^{2+} signal into the mitochondrial matrix (Fülöp et al., 2011) resulting in enhanced aldosterone production (Spät et al., 2012).

In addition to HSL another factor participating in lipolysis, Plin1a (formerly Plin A) has also been detected in Y-1 murine adrenocortical cells (Servetnick et al., 1995). Other Plin isoforms, predominantly Plin1c (formerly Plin C), could also be detected following incubation with cholesterol (Hsieh et al., 2012). Importantly, Plin1a was phosphorylated in a cAMP-dependent manner (Servetnick et al., 1995). The data showing that identical molecules participate in the control of lipid metabolism in adipocytes and adrenocortical cells prompted us to examine whether OPA1, functioning as an AKAP, is a feasible candidate for regulating cAMP-induced steroid secretion. The verified and hypothetical mechanisms supplying cholesterol to mitochondria are shown in Fig. 1. We presumed that silencing of OPA1, if functioning as an AKAP in the extramitochondrial space, would reduce PKA-mediated steroid production to a greater extent than PKA-independent response. Our observations indicate that OPA1 is present in the extramitochondrial compartment in H295R cells but the role of emOPA1 in the control of steroid secretion could not be demonstrated.

2. Materials and methods

2.1. Materials

NIH-H295R cells (ATCC, CRL-2128) were purchased from LGC Standards GmbH, Wesel, Germany. siRNA and silencing RNA products as well as OPTI-MEM, Lipofectamine 2000, Fluo-4 and Mito-Tracker Deep Red were purchased from Life Technologies (Paisley, UK).

Cholesteryl-BODIPY FL C_{12} (C-3927MP) was from Life Technologies (San Diego, CA, USA), UltroSer G was from Bio Septra (Cergy-Saint-Christophe, France). 2mt-eGFP (eGFP fused with a doublet of human cytochrome c oxidase target sequence) was a gift from Dr. B. Enyedi (Budapest, Hungary). Coat-A-Count RIA kit was purchased from Siemens Health Care Diagnostics (Los Angeles, CA).

Primary antibodies were purchased as follows: anti-OPA1 monoclonal antibody (612606): BD Bioscience (Franklin Lakes,

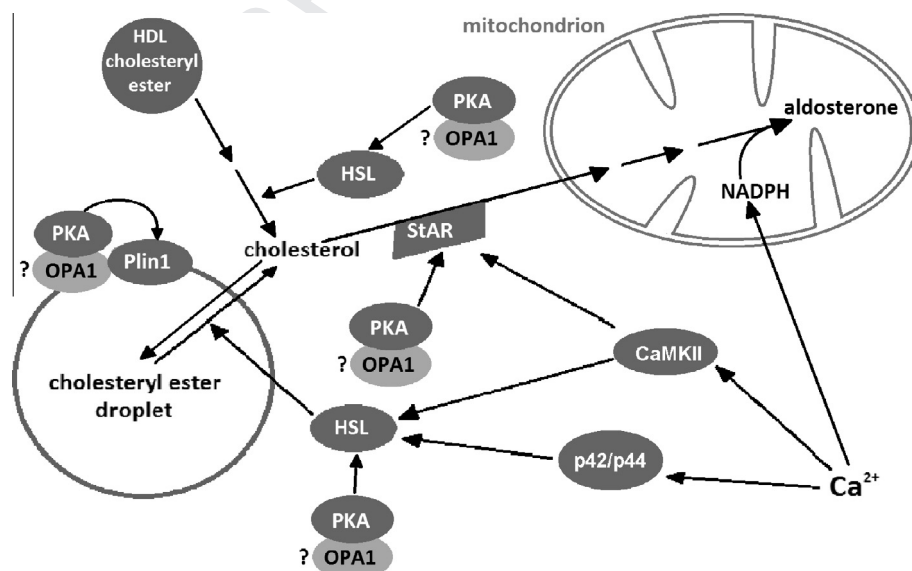


Fig. 1. Cholesterol supply to mitochondria in adrenal glomerulosa cells. The presence and actions of extramitochondrial OPA1 are hypothetical as shown with question marks.

164 NJ); anti-cytochrome oxidase IV (COX IV) monoclonal antibody
165 (SC-58348) and polyclonal antibody (D-20; SC-693599, anti-cyto-
166 chrome c rabbit polyclonal antibody (SC-7159) and HSL monoclo-
167 nal antibody (sc-74489): Santa Cruz Biotechnology (Santa Cruz,
168 CA); anti-protein disulfide isomerase monoclonal antibody
169 (ab2792): Abcam (Cambridge, UK); anti-MFN1 mouse polyclonal
170 antibody (H00055669-M04): Abnova (Taipei, Taiwan) and anti-
171 phospho-HSL rabbit polyclonal antibody (PA5-17488): Thermo Sci-
172 entific (Rockford, IL). Secondary antibodies were as follows: for
173 Western blots: anti-mouse immunoglobulin-HRP: GE Healthcare
174 (Amersham, UK), anti-rabbit immunoglobulin-HRP: GE Health Care
175 Diagnostic (Deerfield, IL) and donkey anti-goat IgG-HRP: Santa
176 Cruz Biotechnology; for immunocytochemistry: Alexa Fluor 568
177 goat anti-mouse IgG (A 11004) and Alexa Fluor 633 goat anti-rab-
178 bit IgG (A 21070): Life Technologies.

179 2.2. Cell culture and transfection

180 H295R cells were grown in DMEM/Ham's F12 (1:1 v/v) contain-
181 ing 1% ITS⁺, 2% UltroSer G, 100 U/ml penicillin and 100 µg/ml strep-
182 tomycin. Passage numbers 4–20 were used. For transfection with
183 2mt-eGFP (for confocal microscopic examination) we used 0.4 µg
184 plasmid DNA with 0.4 µl Lipofectamine 2000 in 220 µl OPTI-
185 MEM medium. The transfection was performed on day 2 and re-
186 peated on day 3. The cells were fixed one day later. For transfection
187 with scrambled RNA or siRNA (for the examination of HSL phos-
188 phorylation and in aldosterone experiments) the cells were elec-
189 troporated before plating, using the Neon electroporator and kit
190 (MPK10025) of Life Technologies. For measuring aldosterone pro-
191 duction the cells were stimulated with appropriate agonists on
192 day 4 (2-h stimulation) or on days 3 and 4 (24-h stimulation).
193 For confocal measurement of [Ca²⁺] the cells were transfected with
194 siRNA on day 2, applying RNAiMax.

195 2.3. Immunocytochemistry

196 For immunocytochemistry about 5 × 10⁴ cells were plated onto
197 glass coverslips. Staining with 2 µM CholEsteryl-BODIPY FL C₁₂ for
198 one day was carried out at 37 °C in CO₂ incubator. The cells were
199 fixed in 4% paraformaldehyde (in PBS, pH 7.4) for 10 min at room
200 temperature and then rinsed. For quenching autofluorescence the
201 samples were incubated in 100 mM glycine for 45 min and then
202 washed twice. Permeabilisation was performed with a mixture of
203 5% milk powder, 0.2% Triton X-100, at room temperature for
204 15 min. Blocking with 5% milk powder, 1% FCS and 0.1% Triton X-
205 100 lasted for 1 h. Incubation with primary antibodies (1:50) in
206 blocking buffer at 4 °C lasted overnight. The secondary antibody
207 (usually at a dilution of 1:100, but for cytochrome c staining Alexa
208 Fluor 633 was diluted 500-fold) was applied in blocking buffer
209 after repeated washings. Further six washings were followed by
210 mounting with MOWIOL.

211 Microscopic examination was undertaken with a Zeiss LSM710
212 confocal laser scanning microscope, operated with ZEN 9.0 soft-
213 ware. The cells were examined with a 63×/1.4 oil immersion
214 objective (Plan-Apochromat, Zeiss). As an exception, for cells trans-
215 fected with 2mt-eGFP a 40×/1.2 water immersion objective (C-
216 Apochromat, Zeiss) was used. Imaging was performed in multi-
217 track mode. The optical slice was 1 µm. The measured cross-over
218 of Alexa 568 into the emission range of Alexa 633 has been sub-
219 tracted applying Image J 1.43u software. The imaging parameters
220 are shown in [Supplementary Table 1](#). Images were deconvoluted
221 with Image J plug-in "Iterative Deconvolve 3D" (Version 5.2). Addi-
222 tional lambda scan imaging was performed with simultaneously
223 acquired emission spectrum of each fluorophore, using array
224 detector.

225 2.4. Cell fractionation

226 2.4.1. Homogenization and mitochondrial fractions

227 Cell fractionation was carried out with three separate sub-
228 clones, first with 3 × 10⁷ and then with 10⁸ cells. Three days after
229 passage the cells were homogenized using microscopic control. A
230 combination of about 40 strokes in a glass-Teflon Potter-Elvjem
231 homogenizer and 40 aspirations and ejections through a 26 gauge
232 needle were applied in a homogenization buffer (50 µl/10⁶ cells)
233 (containing 250 sucrose mM, 10 mM Tris.HCl (pH 7.4), 1 mM EDTA,
234 10 mM NaF, 1 mM benzamidine, 0.075 U/ml Aprotinin, 1 mM PMSF
235 and 1:100 Sigma Mammalian Protease Inhibitor Cocktail) com-
236 pleted with an equal volume of distilled water (total = 1 volume).
237 Following the homogenization the buffer was made isosmotic with
238 the addition of 0.4 volume of a 2.25-fold concentrated homogeni-
239 zation buffer. The homogenate was centrifuged in a swing-out ro-
240 tor at 1000 g_{max} for 10 min. The nuclear pellet was discarded; the
241 supernatant was centrifuged in an Eppendorf fuge (12,000 g_{max}) for
242 15 min. To obtain *mitochondrial* fraction the pellets were pooled,
243 twice resuspended and recentrifuged in homogenation buffer.
244 The resulting pellet was shaken for 30 min at 37 °C in an extracting
245 solution ([Servetnick et al., 1995](#)) and finally spun in the Eppendorf
246 fuge for 15 min. The supernatant, sampled for protein determina-
247 tion, was completed with sample buffer (see below) and stored at
248 –20 °C for analysis on Western blot.

249 2.4.2. Cytosolic fraction

250 The pooled supernatants obtained after the first centrifugation
251 in Eppendorf fuge were transferred into ultracentrifuge tubes and
252 centrifuged in a fixed-angle rotor at 31,000 g_{max} for 25 min. No pel-
253 let was obtained, a sample from the middle height of the tube was
254 withdrawn for protein determination and another aliquot was
255 completed with sample buffer and stored at –20 °C for analysis
256 on Western blot.

257 2.4.3. Fat cake fraction

258 A cloudy aggregate floating in the uppermost layer of the cyto-
259 solic fraction and hence termed fat cake, was aspirated and ex-
260 tracted with 2 vol of extracting solution and processed as done
261 for mitochondria (see above). Samples were withdrawn from the
262 lower phase for protein and Western blot analysis as described
263 for the mitochondrial fraction. Since COX IV concentration of these
264 samples could not be reliably measured, those measured in the
265 cytosolic fraction were used in the calculation of OPA1/COX IV ra-
266 tio. The sample buffer applied for the different cell fractions con-
267 tained the following components, yielding a final concentration
268 given in brackets: Tris.HCl (~40 mM), glycerol (10%), β-mercap-
269 toethanol (5%), bromophenolblue (0.005%) and SDS (2%) (pH 7.0).

270 All the above steps, with exceptions as specified, were per-
271 formed at 4 °C.

272 2.5. Electrophoresis and immunoblotting

273 The cells were suspended in ice-cold lysis buffer (100 mM NaCl,
274 30 mM HEPES pH 7.4, 0.2% Triton X-100, 20 mM NaF, 2.5 mM Na-
275 EGTA, 2.5 mM Na-EDTA, 10 mM benzamidine, 0.075 U/ml Aproti-
276 nin, 1:100 Sigma Mammalian Protease Inhibitor Cocktail, 1 mM so-
277 dium-vanadate, 10 mM PMSF). The insoluble fraction was removed
278 with centrifugation. The supernatant was completed with sample
279 buffer to give a final concentration as described above (Section
280 2.4).

281 Lysed cell samples as well as samples of subcellular fractions
282 were run on 10% (but for HSL 8%) SDS–PAGE and transferred onto
283 nitrocellulose membrane (pore size: 0.45 µm). After blocking, the
284 primary antibodies were applied as follows: cytochrome c
285 (1:200), COX IV (1:200), HSL (1:1000), phospho-HSL (1:500),

Mfn1 (1:500), OPA1 (1:500), PDI (1:3000). Anti-mouse and anti-rabbit secondary antibodies were applied at a dilution of 1:5000 and 1:2500, respectively. For quantitative estimation of OPA1 and COX IV a dilution series of the mitochondrial samples were run parallel with samples of the two supramitochondrial fractions. For quantitative estimation of OPA1 and COX IV a dilution series of the mitochondrial samples were run parallel with samples of the two supramitochondrial fractions. Cytosolic and fat cake samples were compared with mitochondrial samples of comparable optical density on the radiograms. Integral density of regions of interest (ROIs), measured with Image J 1.43u, was corrected for background. The resulting value was regarded as indicator of the amount of separated protein.

2.6. Aldosterone production

For aldosterone experiments the cells were transfected by means of electroporation on day 1 using either equal amounts of three siRNA preparations for *OPA1* (HSS107431, 107432 and 107433) or siRNA for *Mfn1* (5141600) or a 1:1 mixture of non-silencing RNA species with appropriate GC content (12935400 and 129305200). Following electroporation about 2.5×10^5 transfected cells per sample were plated on a 24-well culture dish. The cells were incubated in the tissue culture medium until the 2nd (for 24-h stimulation) or 3rd day (for 2-h stimulation) when the medium was replaced with 0.1% UltroSer G. Next day a 1-h preincubation in serum-free medium was followed by a 2-h or 24-h incubation in the serum-free medium, in the presence of appropriate drugs. Aldosterone content of the incubation medium was measured with Coat-A-Count RIA kit, for calibration synthetic aldosterone was dissolved in cell-free incubation medium.

2.7. Measurement of cytosolic Ca^{2+} concentration

Cells transfected with *Mfn1* or *OPA1* siRNA were examined for $[Ca^{2+}]_c$ three days after transfection. Fluorescence of cells preloaded with Fluo 4 and MitoTracker Deep Red was monitored at room temperature in multitrack mode with Zeiss LSM710 confocal laser scanning microscope, operated with ZEN 11.0 software. The cells were examined with a $63\times/1.4$ oil immersion objective (Plan-Apochromat, Zeiss). Transfection was regarded successful if mitochondria showed fragmented pattern.

2.8. Protein determination

Protein content of cell samples was estimated with Bradford assay for aldosterone measurements and with BCA assay before SDS-PAGE separations.

2.9. Statistics

Means + SEM are shown. For estimating significance of differences unpaired *t*-test, factorial ANOVA and Tukey HSD test (Statistica 11) were used.

3. Results

3.1. Location of OPA1 in H295R cells

The intracellular location of OPA1 was first examined in cells transfected with mitochondrially targeted eGFP (2mt-eGFP). As shown in Fig. 2, mitochondria were immunopositive for OPA1 and a few OPA1 spots could be found also out of the eGFP-labeled

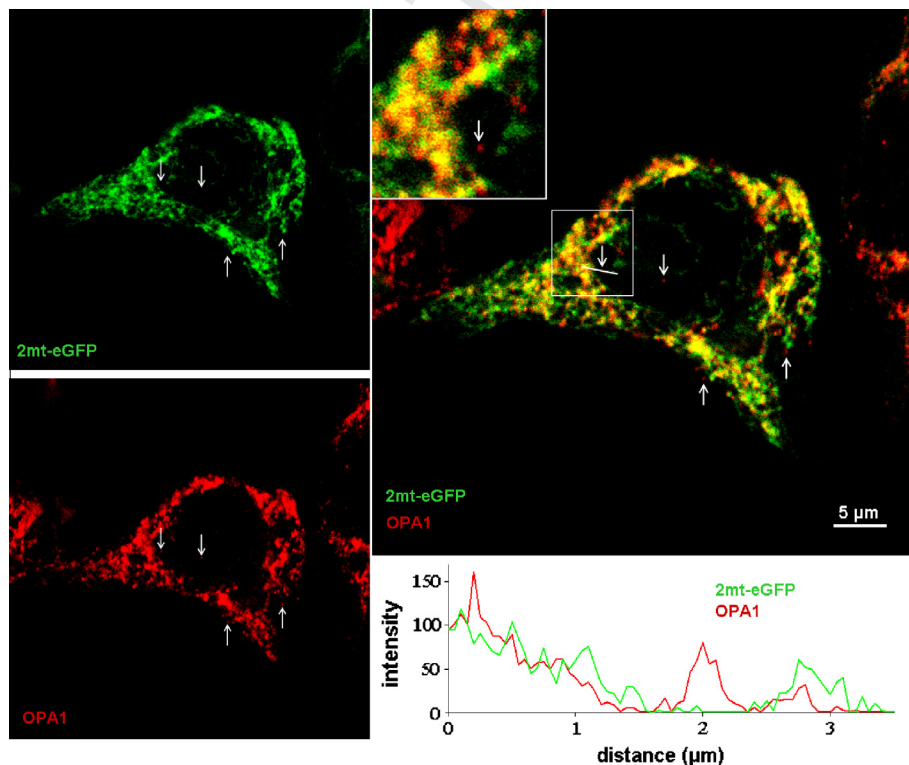


Fig. 2. Confocal microscopic image of immunoreactive OPA1 and mitochondrially targeted eGFP in a H295R cell. OPA1 is shown in red (left lower panel), 2mt-eGFP in green (left upper panel). The merged image is shown in the right upper panel. The arrows point to extramitochondrial OPA1-positive spots. Note that no fluorescence can be seen at the arrowheads in the 2mt-eGFP panel. Intensity (arbitrary units) scanning of the line drawn in the white frame is shown in right-hand lower panel. Representative for 10 out of 21 cells. (For interpretation of the references to colour in this figure legend, the reader is referred to the web version of this article.)

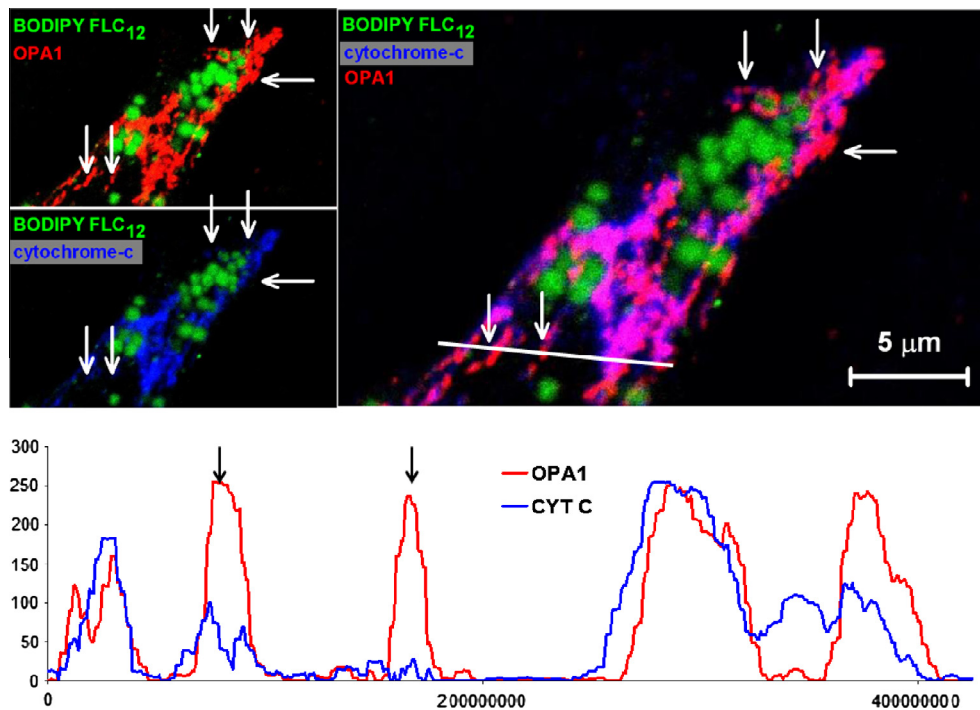


Fig. 3. Confocal microscopic image of cholesterol storing lipid droplets, immunoreactive OPA1 and the IMS-marker cytochrome c in a H295R cell. OPA1 is shown in red and lipid droplets in green (left upper panel), cytochrome c in blue (left lower panel). The right-hand panel shows the merged image. The arrows point to extramitochondrial OPA1-positive spots. Intensity (arbitrary units) scanning of the line drawn in the merged image is shown in the right lower panel. Note that no fluorescence can be seen at the arrowheads in the cytochrome c panel. (Line scanning was performed without prior deconvolution of the image.) Representative for 34 out of 96 cells. (For interpretation of the references to colour in this figure legend, the reader is referred to the web version of this article.)

particles. Altogether, emOPA1 could be detected in 10 out of 21 cells. In order to localize the presumed emOPA1 more precisely, we applied triple staining. Cholesterol storing lipid droplets were stained with the fluorescent cholesterol-ester mimetic CholEsteryl-BODIPY FL C₁₂, OPA1 was immunostained and IMS was labeled with cytochrome c antibody. In average two emOPA1 immunopositive spots have been detected in 34 cells. These spots were mostly located in the vicinity of lipid droplets although OPA1 immunopositivity around the droplets predominantly colocalized with mitochondria (Fig. 3). emOPA1 could not be detected in another 62 cells. No OPA1 immunoreactivity was found after omitting the primary antibody (not shown). Examination with lambda scan mode of confocal microscopy also revealed extramitochondrial immunopositive spots for OPA1 (Supplementary Fig. 1).

3.2. OPA1 in subcellular fractions

The homogenized cells were separated into three fractions by differential centrifugation. Mitochondria were pelleted at 12,000 g_{max} × 15 min. To obtain cytosol the supernatant was centrifuged

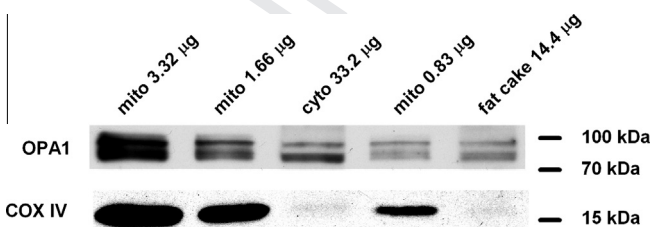


Fig. 4. Western blot analysis of cell fractions. H295R cells were fractionated as detailed in Section 2.4. OPA1 and the IMM-marker COX IV are shown. Representative for 3 cell fractionation studies.

at 31,000 g_{max} × 25 min. A cloudy aggregate floating in the uppermost layer of the cytosolic fraction was withdrawn and termed (in analogy to fat cells) fat cake (Greenberg et al., 1991). The mitochondrial, cytosolic and fat cake fractions were analyzed for OPA1 and the IMM-marker COX IV by Western blotting.

All three fractions contained OPA1 as well as COX IV (Fig. 4 and Supplementary Table 2). In order to estimate mitochondrial contamination, the ratio of OPA1 to COX IV was estimated for all three fractions, taking this ratio in the mitochondrial fraction as unit. The ratio increased in the cytosol over mitochondria by a factor of 11.5 ± 3.5 units ($n = 3$). Due to insufficient amount of protein in one experiment the ratio in the fat cake could be estimated only in two fractionation studies where it attained 26.5 and 33.5 units. These data indicate that the amount of OPA1 in the extramitochondrial fractions was more than attributable to mitochondrial contamination (Supplementary Table 2).

The balance of the long (L) and short (S) isoforms of OPA1 in the cytosolic fraction was shifted towards the short ones as compared to that in the mitochondrial fraction. Whereas the S isoforms may have originated from the IMS of mitochondria with damaged OMM, L isoforms, which are anchored to the IMM (Delettre et al., 2000; Lenaers et al., 2009; Liesa et al., 2009), may not have such an origin. The contamination of the post-mitochondrial fractions with cytochrome c (Supplementary Table 2) supports the assumption that S isoforms may originate from damaged mitochondria.

3.3. Effect of OPA1 silencing on HSL phosphorylation

In order to test the presumed AKAP function of OPA1 we examined the knock-down of OPA1 on phosphorylation of HSL, a major target of PKA. Exposing the cells to db-cAMP for 2 h brought about a concentration dependent increase in the phosphorylated fraction of the enzyme ($p = 0.0009$). Although the mean extent of phosphorylation was somewhat lower in cells transfected with OPA1 siRNA

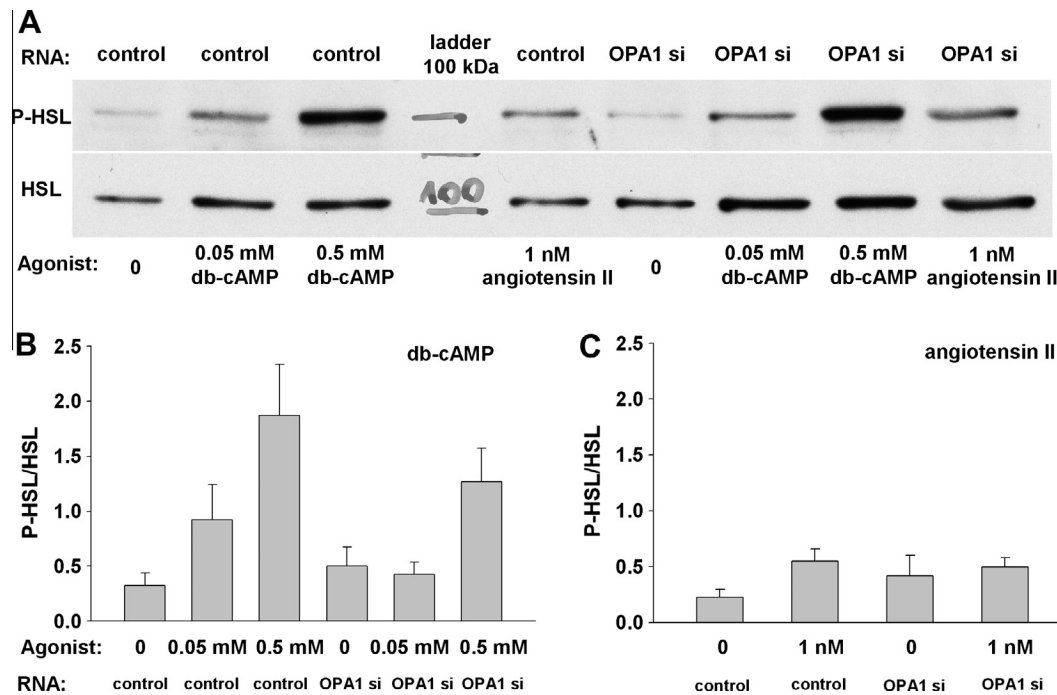


Fig. 5. Effect of knock-down of *OPA1* on phosphorylation of hormone-sensitive lipase (HSL) by 2-h stimulation with db-cAMP (0.05 or 0.5 mM) or 1 nM angiotensin II (angio). (A) The Western blot shows phosphorylated (upper panel) and total HSL (lower panel) on the same membrane. Statistics are shown for the effect of db-cAMP ($n = 5$) (B) and angiotensin II ($n = 4$) (C). The ordinates show the quotients of phosphorylated and total HSL densities. The effect of *OPA1* siRNA was not significant (ANOVA, $p = 0.19$).

(Fig. 5 and Supplementary Fig. 2), the effect of silencing was not statistically significant ($p = 0.19$).

Next we examined whether angiotensin II-induced phosphorylation of HSL was dependent on *OPA1*. The hormone (1 nM) doubled the formation of phospho-HSL. The knock-down of *OPA1* was without effect (Fig. 5).

3.4. Effect of *OPA1* silencing on cAMP-induced Ca^{2+} signaling

Eighty-five *Mfn1*-silenced cells and 52 *OPA1*-silenced cells were stimulated with 0.05 mM db-cAMP. Most of the cells failed to respond within 10 min. The evaluable response in 7 control cells was almost thrice as high as that in 3 *OPA1*-silenced cells; however, the number of responsive cells was too low for obtaining any conclusion. When the cells were stimulated with 0.5 mM db-cAMP, 8 out of 42 *Mfn1*-silenced cells and 9 out of 39 *OPA1*-silenced cells exhibited characteristic Ca^{2+} signal, with a lag-time between 4 and 10 min. Silencing failed to modify the amplitude of Ca^{2+} peaks (Supplementary Fig. 3).

3.5. Effect of *OPA1* silencing on aldosterone production

In order to ascertain whether emOPA1 exerts any effect on cholesterol supply of steroid production we examined the effect of *OPA1* silencing on the PKA-dependent aldosterone production. Considering that siRNA for *OPA1* induces fragmentation of mitochondria (Olichon et al., 2003) and the consecutive changes in mitochondrial volume/surface ratio might influence signaling processes, comparison with maintained *OPA1* expression but fragmented mitochondria were also required. Knock-down of *Mfn1* also induces fragmentation without changes in the structure of IMM (Arnoult et al., 2005; Eura et al., 2003). Transfection with siRNA for *OPA1* in H295R cells efficiently reduced the expression of *OPA1* protein and did not influence that of *Mfn1* protein (Fig. 1 in Fülöp et al., 2011) whereas transfection with siRNA for *Mfn1* exerted reciprocal effect (not shown). Knock-down of *OPA1* and *Mfn1*

induce fragmentation with indistinguishable morphometric changes (Figs. S1 and S3 in Fülöp et al., 2011) therefore, in addition to the effect of transfection with scrambled RNA the effect of siRNA against *Mfn1* on hormone production has also been examined.

Aldosterone production has been studied under two different conditions. During acute (2-h) stimulation with db-cAMP or angiotensin II hormone production depends on the activation of the mechanism transporting cholesterol to the IMM. In contrast, during long-term stimulation several proteins participating in hormone production are also synthesized (Coulombe et al., 1996; Hattangady et al., 2011; Spät and Hunyady, 2004). The greatly enhanced steroid production will then be much more dependent on available free cholesterol.

Aldosterone response to db-cAMP or angiotensin II was examined in cells transfected with either control RNA or *Mfn1* siRNA or *OPA1* siRNA. Each group was stimulated with either 0.05 or 0.5 mM db-cAMP or 1 nM angiotensin II for 2 h or with 0.5 mM db-cAMP or 10 nM angiotensin II for 24 h. Qualitatively similar aldosterone responses were measured in the short and long-term stimulation series. db-cAMP stimulated aldosterone production in each group in a concentration-dependent way. Comparison of aldosterone production rates after transfection with various RNA species showed that highest responses were attained in the *OPA1*-silenced cells (for the effect of *OPA1* siRNA: $p = 10^{-4}$) (Fig. 6 and 7). Importantly, knock-down of *OPA1* equally affected the response to db-cAMP and angiotensin II, related to the effect of either type of control transfection (Table 1). These measurements indicate that the effect of *OPA1* siRNA does not depend on the involvement of PKA in the stimulation of aldosterone production.

4. Discussion

Mitochondrial protein *OPA1* located in close proximity with the lipid droplets has recently been described in lipocytes (Pidoux et al., 2011). Functioning as an AKAP it amplifies the PKA-induced phosphorylation of Plin 1, thus permitting enhanced lipolytic ac-

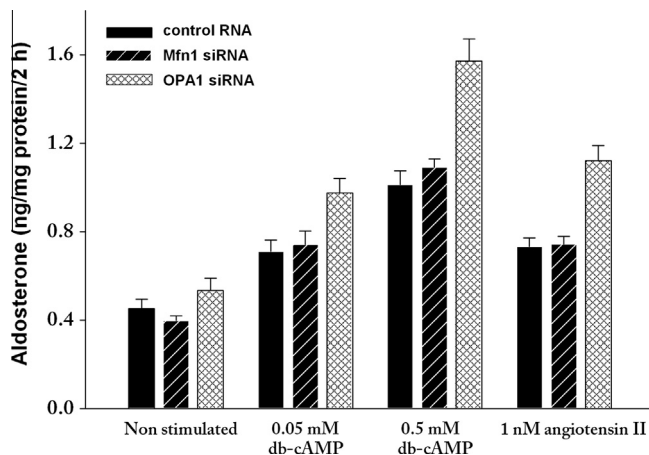


Fig. 6. Effect of knock-down of *OPA1* on short-term aldosterone production. The cells were transfected by means of electroporation with scrambled RNA or siRNA against *OPA1* or *Mfn1* before plating. (Knock-down of *Mfn1* evokes mitochondrial fragmentation similar to the effect of siRNA for *OPA1*.) Three days later the cells were stimulated with db-cAMP (0.05 or 0.5 mM) or angiotensin II (1 nM) for 2 h. Mean + SEM of 6 experiments derived from 3 separate cell passages are shown. The effect of agonists and that of RNA were highly significant (ANOVA, $p < 10^{-6}$). Highest aldosterone responses were attained in the *OPA1*-silenced cells (Tukey test, $p = 10^{-4}$).

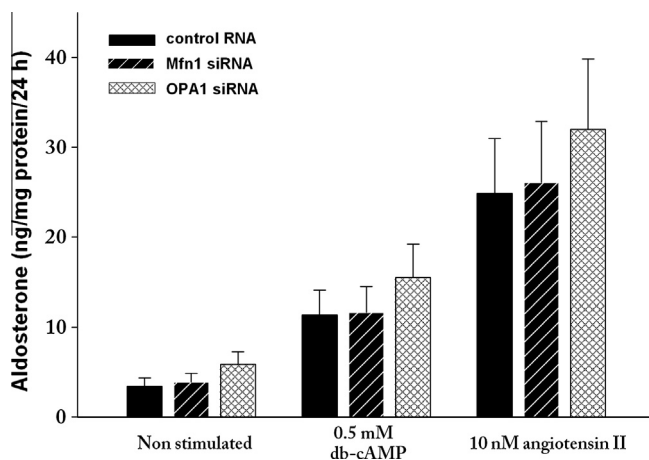


Fig. 7. Effect of knock-down of *OPA1* on long-term aldosterone production. The cells were transfected as described for Fig. 6, however, two days after plating the cells were stimulated with db-cAMP (0.5 mM) or angiotensin II (10 nM) for 24 h. Mean + SEM of 6 experiments derived from 4 separate cell passages are shown. The effect of agonists and that of RNA were highly significant (ANOVA, $p < 10^{-6}$). Highest aldosterone responses were attained in the *OPA1*-silenced cells (Tukey test, $p = 10^{-4}$).

tion of HSL (Greenberg et al., 2011; Pidoux et al., 2011). HSL is a major or sole factor responsible for cholesterol esterase activity in steroid producing tissues including the adrenal cortex (Kraemer et al., 2004). Plin 1 has been detected in a murine adrenocortical cell line (Servetnick et al., 1995). In analogy to lipocytes (Brasaemle et al., 2009; Sztalryd et al., 2003; Zhang et al., 2003) it can be

hypothetised that also in adrenocortical cells, under control conditions, Plin 1 forms a barrier at the surface of cholesterol ester containing lipid droplets. Upon activation of PKA both HSL and Plin 1 undergo phosphorylation, the phosphorylated HSL docks to the Plin 1 and gains access to cholesterol esters (Fig. 1). Presently no data are available whether *OPA1* exists in the cytosol of adrenocortical cells and whether, functioning as an AKAP, it enhances cAMP-induced aldosterone secretion.

When the cells are stimulated with a cAMP-mediated agonist, PKA may enhance cholesterol supply of mitochondria primarily by inducing and phosphorylating the cholesterol transporter StAR and the translocator protein TSPO (Holysz et al., 2011; Midzak et al., 2011). It may be assumed that without simultaneous activation of HSL StAR would function without substrate saturation. In fact, PKA phosphorylates also HSL (Hirsch and Rosen, 1984). Therefore HSL action on cytosolic cholesterol esters imported from the extracellular fluid as well as on those stored in lipid droplets (Hattangady et al., 2011; Rone et al., 2009; Vinson et al., 1992) may optimize cholesterol supply of mitochondria. Moreover, provided data can be extrapolated from adipocytes (Miyoshi et al., 2006), PKA phosphorylates perilipin and thereby facilitates the access of activated HSL to its substrate. If *OPA1* is present in the extramitochondrial space, due to its AKAP domain it could enhance most or all of these processes. Moreover, even if HSL activity does not limit hormone production, induction and activation of StAR is cAMP - PKA dependent, therefore the elimination of the AKAP function could still be reflected by attenuated cAMP - induced aldosterone production.

As a first approach to detect emOPA1 we applied immunocytochemical technique, using laser scanning confocal microscopy. In the first series *OPA1* was immunolabeled and mitochondria were identified with mitochondrially targeted eGFP. In two further series immunostaining was applied to *OPA1* as well as to cytochrome c, a mitochondrial marker located in the IMS whereas the lipid droplets were stained with the cholesterol ester analogue Cholesteryl-BODIPY. The overwhelming majority of *OPA1* positive spots around the droplets colocalized with mitochondria. A few emOPA1 immunopositive spots could also be found, mostly but not exclusively in the vicinity of lipid droplets. Overall, nearly 40 per cent of cells displayed emOPA1 immunopositivity but the density of such signals was almost negligible. Therefore in spite of its presence in the extramitochondrial space it was dubious whether at such a low density in this space *OPA1* can influence cholesterol and thereby steroid metabolism.

Cell fractionation studies yielded similar results. Three fractions were analyzed by means of Western blotting, the mitochondrial and cytosolic fractions as well as the uppermost layer of the cytosolic fraction, termed fat cake. This latter fraction contained a floating cloudy aggregate, probably corresponding to the lipid droplet-rich fat cake in the cytosolic fraction of lipocytes (Greenberg et al., 1991). Mitochondrial contamination of the post-mitochondrial fractions was estimated on basis of their COX IV and cytochrome c content, markers of IMM and IMS, respectively. The clear-cut increase of *OPA1*/COX IV ratio in the cytosolic and fat cake fractions indicated the presence of *OPA1* in the extramitochondrial compartment. The negligible amount of COX IV argues against the

Table 1

Aldosterone production by *OPA1* - silenced cells, related to that by cells transfected with control RNA or *Mfn1* siRNA.

| Agonist | 2 h | | 24 h | |
|----------------------|---------------|-------------------|---------------|-------------------|
| | Control RNA | <i>Mfn1</i> siRNA | Control RNA | <i>Mfn1</i> siRNA |
| 0.05 mM db-cAMP | 1.400 ± 0.138 | 1.340 ± 0.131 | | |
| 0.5 mM db-cAMP | 1.580 ± 0.150 | 1.450 ± 0.114 | 1.367 ± 0.072 | 1.356 ± 0.076 |
| 1 nM angiotensin II | 1.555 ± 0.128 | 1.514 ± 0.094 | | |
| 10 nM angiotensin II | | | 1.289 ± 0.012 | 1.292 ± 0.063 |

assumption that mitochondrial contamination is a major factor accounting for the presence of OPA1 in the post-mitochondrial fractions. Unexpectedly, the pattern of OPA1 isoforms in the mitochondrial fraction differed from that in the post-mitochondrial fractions, being relatively enriched in short isoforms in the latter ones. Since long isoforms are strongly attached to the IMM by their transmembrane domain whereas the short isoforms, lacking transmembrane domain 1 (Song JCB 2007) are only weakly attached to membranes (Satoh et al., 2003), the damage of the OMM may lead to the leakage of short isoforms only. (Note that only a small fraction of cytochrome *c* is bound to membranes (Cortese et al., 1998), therefore its leakage may exceed that of short OPA1 isoforms.) The presence of cytochrome *c* in the cytosol supports the assumption that OMM damage of variable extent may have occurred during cell homogenization.

Since immunocytochemical and cell fractionation studies failed to provide unambiguous indication for the significance of emOPA1 we examined the effect of OPA1 siRNA on three PKA targets, namely HSL, the cAMP-evoked Ca²⁺ signaling and aldosterone production.

Two-hour stimulation with db-cAMP significantly enhanced the phosphorylation of HSL. Transfection with OPA1 siRNA was followed by a slight, statistically insignificant decrease in the mean value of phosphorylation. Angiotensin II-induced phosphorylation of HSL, accounted for by Ca²⁺ dependent activation of CaMKII (Cherradi et al., 1998) was not sensitive to OPA1 siRNA.

ACTH as well as 8-bromo-cAMP induce sustained Ca²⁺ response after a lag-time of a few minutes in rat (Tremblay et al., 1991) and human glomerulosa cells (Gallo-Payet et al., 1996). Similarly to myocardial cells (Sperelakis and Schneider, 1976) this effect of cAMP in glomerulosa cells is brought about by the phosphorylation of L-type Ca²⁺ channels by PKA (Durroux et al., 1991). It follows that cAMP-induced Ca²⁺ signal could be regarded as an indicator of OPA1 functioning as an extramitochondrial AKAP. db-cAMP-induced Ca²⁺ signal in small fraction of the cells only. The signal developed after a lag-time of several minutes and in quite a few cases it was not substantial enough for reliable measurement. For these reasons the effect of OPA1 silencing on the effect of 0.05 mM db-cAMP could not be conclusively evaluated. At a higher concentration (0.5 mM) of the agonist, one third of the cells displayed Ca²⁺ signal and it was resistant to silencing of OPA1.

Irrespective of any effect of OPA1 on HSL in cAMP activated cells, its presumed action on PKA should facilitate phosphorylation and induction of StAR that in turn should lead to increased steroid production. Moreover, the biological significance of OPA1 in H295R cells depends should be indicated on by its effect on aldosterone secretion. Although aldosterone is one of several steroids produced by H295R cells, all these steroids derive from the same cholesterol pool and therefore aldosterone can be regarded as an appropriate indicator of mitochondrial access to cholesterol. At designing the experiments it had to be recalled that siRNA for OPA1 evokes fragmentation of mitochondria. In H295R cells the mitochondrion fragmenting effect of *Mfn1* siRNA is comparable with that of OPA1 siRNA (Fülöp et al., 2011), therefore cells transfected with siRNA against *Mfn1* were considered the appropriate control.

In principle, silencing of OPA1 might exert a dual action on aldosterone production, depending on the mode of action (cAMP or Ca²⁺) of the physiological agonist. Although angiotensin II is a Ca²⁺ mobilizing agonist and the action of ACTH is mediated by cAMP, there is some overlap between their mode of action. Angiotensin II, acting via the heterotrimeric G-protein G_q (Gutowski et al., 1991), induces acute aldosterone secretion by IP₃-mediated Ca²⁺ release (Enyedi et al., 1985), followed by Ca²⁺ influx (Hunyady et al., 1994; Kramer, 1988). The ensuing Ca²⁺ signal is a prerequisite for increased aldosterone secretion (Spät and Hunyady, 2004). ACTH or cAMP may also induce Ca²⁺ influx and this Ca²⁺

influx contributes to the stimulation of aldosterone (Balla et al., 1982). Ca²⁺ influx may be attributed to PKA-enhanced activation of L-type Ca²⁺ channels (Gallo-Payet et al., 1996; Lenglet et al., 2002). db-cAMP-induced Ca²⁺ signals were observed also in the present experiments. It follows that Ca²⁺ signaling may be a common element in the action of angiotensin II and cAMP. In contrast to Ca²⁺ signaling, cAMP is not a common mediator of the two agonists. In addition to G_q angiotensin II also activates the adenylyl cyclase inhibitory G protein G_i (Enyedi et al., 1986; Maturana et al., 1999). This may be the reason why the peptide does not increase the generation of cAMP (Bell et al., 1981; Hausdorff et al., 1987) despite the probable expression (Tait and Tait, 1999) of Ca²⁺ sensitive isoforms of adenylyl cyclase (Hanoune and Defer, 2001).

Cytosolic Ca²⁺ signal is transferred into the mitochondrial matrix (Hajnoczky et al., 1995; Pralong et al., 1992; Rizzuto et al., 1992) and the elevated mitochondrial [Ca²⁺] contributes to the enhancement of steroid production (Spät et al., 2012; Wiederkehr et al., 2011). Therefore changes in mitochondrial Ca²⁺ metabolism should be considered at evaluating the effect of OPA1 knockdown on aldosterone production. Applying the mitochondrially targeted Ca²⁺-sensitive proteins 4mt-D2 and mt-inverse Pericam we observed that knockdown of OPA1 significantly enhanced mitochondrial Ca²⁺ uptake both in intact and permeabilized H295R and HeLa cells (Fülöp et al., 2011). This enhancement was associated with increased aldosterone production (Spät et al., 2012). Our data on HeLa cells have not been confirmed by Kushnareva et al. (2012) who estimated [Ca²⁺]_m with Rhod-2, a dye less specific for mitochondria than the mitochondrially targeted proteins applied in our experiments. Alluding to the increased circularity (a parameter indicating fragmentation) of mitochondria in the OPA1-silenced cells (Fülöp et al., 2011) Kushnareva et al. attributed our results to swelling of mitochondria. It should, however, be recalled that we observed enhanced Ca²⁺ uptake also in comparison with *Mfn1*-silenced cells, displaying circularity identical with that in OPA1-silenced cells. Kushnareva et al. also reported that the number of Ca²⁺ pulses required to activate mitochondrial permeability transition pore is less in OPA1-silenced cells than in sham-transfected controls. This observation may indicate enhanced rather than attenuated Ca²⁺ uptake (cf. e.g. Joiner et al., 2012; Mallilankaraman et al., 2012)). In addition to increased mitochondrial Ca²⁺ uptake knock-down of OPA1 may enhance aldosterone production also by enhanced cholesterol transport through the IMM into the matrix, as observed in trophoblast cells (Wasilewski et al., 2012).

Again, in contrast to Ca²⁺ signaling, cAMP is not a common intracellular mediator of ACTH and AII. Therefore, in OPA1-silenced cells, due to the elimination of the presumed AKAP function, the amplification of secretory response to db-cAMP should be smaller than in angiotensin II-stimulated cell. Nevertheless, this was not the case. In fact, silencing of OPA1 the fold-response to all the stimuli increased in each group to the same extent, irrespective whether PKA participated in the activation of steroid production. This indicates that AKAP action of OPA1 has no role in the activation of cAMP-PKA mediated hormone production.

A special member of the AKAP family, AKAP121 can be anchored to mitochondria and may compartmentalize PKA as well as other proteins on the OMM (Wong and Scott, 2004). In Leydig cells, cAMP-induced StAR expression and steroidogenesis were found to correlate with the extent of AKAP 121 expression (Dyson et al., 2008). Expression and role of AKAP121 in H295R cells deserve elucidation.

In a recent review on OPA1 Belenguer and Pellegrini (Belenguer and Pellegrini, 2012) emphasized the possibility that OPA1 reported to be present in the lipid droplet fraction of adipocytes (Pidoux et al., 2011) may have been due to contamination with mitochondria. These authors raised several questions concerning the proposed role of OPA1 in lipolysis. Our observations support

648 the presence of OPA1 in the extramitochondrial space, for the first
649 time in a cell type other than adipocyte. At the same time we ob-
650 tained no evidence for the role of this fraction of OPA1 in cAMP-
651 mediated steroid hormone production, the specific biological func-
652 tion of adrenocortical cells.

653 Acknowledgements

654 This work was supported by the Hungarian Council for Medical
655 Research (ETT 008-09). The excellent technical assistance of Ms.
656 Eszter Halász is highly appreciated.

657 Appendix A. Supplementary material

658 Supplementary data associated with this article can be found, in
659 the online version, at <http://dx.doi.org/10.1016/j.mce.2013.07.021>.

660 References

- 661 Arnoult, D., Grodet, A., Lee, Y.J., Estaquier, J., Blackstone, C., 2005. Release of OPA1
662 during apoptosis participates in the rapid and complete release of cytochrome c
663 and subsequent mitochondrial fragmentation. *J. Biol. Chem.* 280, 35742–35750.
664 Balla, T., Hunyady, L., Spät, A., 1982. Possible role of calcium uptake and calmodulin
665 in adrenal glomerulosa cells: effects of verapamil and trifluoperazine. *Biochem.*
666 *Pharmacol.* 31, 1267–1271.
667 Belenguer, P., Pellegrini, L., 2012. The dynamin GTPase OPA1: more than
668 mitochondria? *Biochim. Biophys. Acta* 1833, 176–183.
669 Bell, J.B.G., Tait, J.F., Tait, S.A.S., Barnes, G.D., Brown, B.L., 1981. Lack of effect of
670 angiotensin on levels of cyclic AMP in isolated adrenal zona glomerulosa cells
671 from the rat. *J. Endocrinol.* 91, 145–154.
672 Betancourt-Calle, S., Calle, R.A., Isaacs, C.M., White, S., Rasmussen, H., Bollag, W.B.,
673 2001. Differential effects of agonists of aldosterone secretion on steroidogenic
674 acute regulatory phosphorylation. *Mol. Cell. Endocrinol.* 173, 87–94.
675 Brasaemle, D.L., Subramanian, V., Garcia, A., Marcinkiewicz, A., Rothenberg, A., 2009.
676 Perilipin A and the control of triacylglycerol metabolism. *Mol. Cell Biochem.*
677 326, 15–21.
678 Cherradi, N., Brandenburger, Y., Capponi, A.M., 1998. Mitochondrial regulation of
679 mineralocorticoid biosynthesis by calcium and the StAR protein. *Eur. J.*
680 *Endocrinol.* 139, 249–256.
681 Cherradi, N., Pardo, B., Greenberg, A.S., Kraemer, F.B., Capponi, A.M., 2003.
682 Angiotensin II activates cholesterol ester hydrolase in bovine adrenal
683 glomerulosa cells through phosphorylation mediated by p42/p44 mitogen-
684 activated protein kinase. *Endocrinology* 144, 4905–4915.
685 Cipolat, S., Martins, D.B., Dal Zilio, B., Scorrano, L., 2004. OPA1 requires mitofusin 1
686 to promote mitochondrial fusion. *Proc. Natl. Acad. Sci. USA* 101, 15927–15932.
687 Clark, B.J., Pezzi, V., Stocco, D.M., Rainey, W.E., 1995. The steroidogenic acute
688 regulatory protein is induced by angiotensin II and K⁺ in H295R adrenocortical
689 cells. *Mol. Cell. Endocrinol.* 115, 215–219.
690 Cortese, J.D., Voglino, A.L., Hackenbrock, C.R., 1998. Multiple conformations of
691 physiological membrane-bound cytochrome c. *Biochemistry* 37, 6402–6409.
692 Coulombe, N., Lefebvre, A., Lehoux, J.G., 1996. Characterization of the hamster
693 CYP11B2 gene regulatory regions. *Endocr. Res.* 22, 653–661.
694 Delettre, C., Lenaers, G., Griffoin, J.M., Gigarel, N., Lorenzo, C., Belenguer, P.,
695 Pelloquin, L., Grosgeorge, J., Turc-Carel, C., Perret, E., Astarie-Dequeker, C.,
696 Lasquell, L., Arnaud, B., Ducommun, B., Kaplan, J., Hamel, C.P., 2000. Nuclear
697 gene OPA1, encoding a mitochondrial dynamin-related protein, is mutated in
698 dominant optic atrophy. *Nat. Genet.* 26, 207–210.
699 Durroux, T., Gallo-Payet, N., Payet, M.D., 1991. Effects of adrenocorticotropin on
700 action potential and calcium currents in cultured rat and bovine glomerulosa
701 cells. *Endocrinology* 129, 2139–2147.
702 Dyson, M.T., Jones, J.K., Kowalewski, M.P., Manna, P.R., Alonso, M., Gottesman, M.E.,
703 Stocco, D.M., 2008. Mitochondrial A-kinase anchoring protein 121 binds type II
704 protein kinase A and enhances steroidogenic acute regulatory protein-mediated
705 steroidogenesis in MA-10 mouse Leydig tumor cells. *Biol. Reprod.* 78, 267–277.
706 Enyedi, P., Büki, B., Mucsi, I., Spät, A., 1985. Polyphosphoinositide metabolism in
707 adrenal glomerulosa cells. *Mol. Cell. Endocrinol.* 41, 105–112.
708 Enyedi, P., Mucsi, I., Hunyady, L., Catt, K.J., Spät, A., 1986. The role of guanyl
709 nucleotide binding proteins in the formation of inositol phosphates in adrenal
710 glomerulosa cells. *Biochem. Biophys. Res. Commun.* 140, 941–947.
711 Eura, Y., Ishihara, N., Yokota, S., Mihara, K., 2003. Two mitofusin proteins,
712 mammalian homologues of FZO, with distinct functions are both required for
713 mitochondrial fusion. *J. Biochem.* 134, 333–344.
714 Fleury, A., Mathieu, A.P., Ducharme, L., Hales, D.B., Lehoux, J.G., 2004.
715 Phosphorylation and function of the hamster adrenal steroidogenic acute
716 regulatory protein (StAR). *J. Steroid Biochem. Mol. Biol.* 91, 259–271.
717 Frey, T.G., Renken, C.W., Perkins, G.A., 2002. Insight into mitochondrial structure
718 and function from electron tomography. *Biochim. Biophys. Acta* 1555, 196–203.
719 Fülöp, L., Szanda, G., Enyedi, B., Várnai, P., Spät, A., 2011. The effect of OPA1 on
720 mitochondrial Ca²⁺ signaling. *PLoS One* 6, e25199.

- Gallo-Payet, N., Grazzini, E., C⁺t, M., Chouinard, L., Chorvatova, A., Bilodeau, L., Payet, M.D., Guillon, G., 1996. Role of Ca²⁺ in the action of adrenocorticotropin in cultured human adrenal glomerulosa cells. *J. Clin. Invest.* 98, 460–466.
722
723
724 Granneman, J.G., Moore, H.P., 2008. Location, location: protein trafficking and lipolysis in adipocytes. *Trends Endocrinol. Metab.* 19, 3–9.
725
726 Granneman, J.G., Moore, H.P., Mottillo, E.P., Zhu, Z., Zhou, L., 2011. Interactions of perilipin-5 (Plin5) with adipose triglyceride lipase. *J. Biol. Chem.* 286, 5126–5135.
727
728
729 Greenberg, A.S., Egan, J.J., Wek, S.A., Garty, N.B., Blanchette-Mackie, E.J., Londos, C., 1991. Perilipin, a major hormonally regulated adipocyte-specific phosphoprotein associated with the periphery of lipid storage droplets. *J. Biol. Chem.* 266, 11341–11346.
730
731
732 Greenberg, A.S., Kraemer, F.B., Soni, K.G., Jedrychowski, M.P., Yan, Q.W., Graham, C.E., Bowman, T.A., Mansur, A., 2011. Lipid droplet meets a mitochondrial protein to regulate adipocyte lipolysis. *EMBO J.* 30, 4337–4339.
733
734
735 Gutowski, S., Smrcka, A., Nowak, L., Wu, D., Simon, M., Sternweis, P.C., 1991. Antibodies to the alpha_q subfamily of guanine nucleotide-binding regulatory protein β subunits attenuate activation of phosphatidylinositol 4,5-bisphosphate hydrolysis by hormones. *J. Biol. Chem.* 266, 20519–20524.
736
737
738 Hajnóczky, G., Robb-Gaspers, L.D., Seitz, M.B., Thomas, A.P., 1995. Decoding of cytosolic calcium oscillations in the mitochondria. *Cell* 82, 415–424.
739
740
741 Hanoune, J., Defer, N., 2001. Regulation and role of adenylyl cyclase isoforms. *Annu. Rev. Pharmacol. Toxicol.* 41, 145–174.
742
743
744 Hattangady, N.G., Olala, L.O., Bollag, W.B., Rainey, W.E., 2011. Acute and chronic regulation of aldosterone production. *Mol. Cell Endocrinol.*
745
746 Hausdorff, W.P., Sekura, R.D., Aguilera, G., Catt, K.J., 1987. Control of aldosterone production by angiotensin II is mediated by two guanine nucleotide regulatory proteins. *Endocrinology* 120, 1668–1678.
747
748
749 Hirsch, A.H., Rosen, O.M., 1984. Lipolytic stimulation modulates the subcellular distribution of hormone-sensitive lipase in 3T3-L1 cells. *J. Lipid Res.* 25, 665–677.
750
751
752 Holm, C., Osterlund, T., Laurell, H., Contreras, J.A., 2000. Molecular mechanisms regulating hormone-sensitive lipase and lipolysis. *Annu. Rev. Nutr.* 20, 365–393.
753
754 Holysz, M., Derebecka-Holysz, N., Trzeciak, W.H., 2011. Transcription of LIPE gene encoding hormone-sensitive lipase/cholesteryl esterase is regulated by SF-1 in human adrenocortical cells: involvement of protein kinase A signal transduction pathway. *J. Mol. Endocrinol.* 46, 29–36.
755
756
757 Hsieh, K., Lee, Y.K., Londos, C., Raaka, B.M., Dalen, K.T., Kimmel, A.R., 2012. Perilipin family members preferentially sequester to either triacylglycerol-specific or cholesteryl-ester-specific intracellular lipid storage droplets. *J. Cell Sci.* 125, 4067–4076.
758
759
760 Hunyady, L., Rohács, T., Bagó, A., Deák, Spät, A., 1994. Dihydropyridine-sensitive initial component of the ANG II-induced Ca²⁺ response in rat adrenal glomerulosa cells. *Am. J. Physiol. Cell Physiol.* 266, C67–C72.
761
762
763 Joiner, M.L., Koval, O.M., Li, J., He, B.J., Allamargot, C., Gao, Z., Luczak, E.D., Hall, D.D., Fink, B.D., Chen, B., Yang, J., Moore, S.A., Scholz, T.D., Strack, S., Mohler, P.J., Sivitz, W.I., Song, L.S., Anderson, M.E., 2012. CaMKII determines mitochondrial stress responses in heart. *Nature* 491, 269–273.
764
765
766 Kraemer, F.B., Shen, W.J., Harada, K., Patel, S., Osuga, J., Ishibashi, S., Azhar, S., 2004. Hormone-sensitive lipase is required for high-density lipoprotein cholesteryl ester-supported adrenal steroidogenesis. *Mol. Endocrinol.* 18, 549–557.
767
768
769 Kramer, R.E., 1988. Angiotensin II-stimulated changes in calcium metabolism in cultured glomerulosa cells. *Mol. Cell. Endocrinol.* 60, 199–210.
770
771
772 Kushnareva, Y.E., Gerencser, A.A., Bossy, B., Ju, W.K., White, A.D., Waggoner, J., Ellisman, M.H., Perkins, G., Bossy-Wetzel, E., 2012. Loss of OPA1 disturbs cellular calcium homeostasis and sensitizes for excitotoxicity. *Cell Death Differ.*
773
774
775 Lenaers, G., Reynier, P., Elachouri, G., Soukkaiech, C., Olichon, A., Belenguer, P., Baricault, L., Ducommun, B., Hamel, C., Delettre, C., 2009. OPA1 functions in mitochondria and dysfunctions in optic nerve. *Int. J. Biochem. Cell Biol.* 41, 1866–1874.
776
777
778 Lenglet, S., Louiset, E., Delarue, C., Vaudry, H., Cousse, V., 2002. Activation of 5-HT(7) receptor in rat glomerulosa cells is associated with an increase in adenylyl cyclase activity and calcium influx through T-type calcium channels. *Endocrinology* 143, 1748–1760.
779
780
781 Liesa, M., Palacin, M., Zorzano, A., 2009. Mitochondrial dynamics in mammalian health and disease. *Physiol. Rev.* 89, 799–845.
782
783
784 Lucki, N.C., Bandyopadhyay, S., Wang, E., Merrill, A.H., Sewer, M.B., 2012. Acid ceramidase (ASA1) is a global regulator of steroidogenic capacity and adrenocortical gene expression. *Mol. Endocrinol.* 26, 228–243.
785
786
787 Mallilankaraman, K., Doonan, P., Cardenas, C., Chandramoorthy, H.C., Muller, M., Miller, R., Hoffman, N.E., Gandhirajan, R.K., Molgo, J., Birnbaum, M.J., Rothberg, B.S., Mak, D.O., Foscett, J.K., Madesh, M., 2012. MICU1 is an essential gatekeeper for MCU-mediated mitochondrial Ca²⁺ uptake that regulates cell survival. *Cell* 151, 630–644.
788
789
790 Manna, P.R., Dyson, M.T., Eubank, D.W., Clark, B.J., Lalli, E., Sassone-Corsi, P., Zelezniak, A.J., Stocco, D.M., 2002. Regulation of steroidogenesis and the steroidogenic acute regulatory protein by a member of the cAMP response-element binding protein family. *Mol. Endocrinol.* 16, 184–199.
791
792
793 Martin, L.J., Boucher, N., Brousseau, C., Tremblay, J.J., 2008. The orphan nuclear receptor NUR77 regulates hormone-induced StAR transcription in Leydig cells through cooperation with Ca²⁺/calmodulin-dependent protein kinase I. *Mol. Endocrinol.* 22, 2021–2037.
794
795
796 Maturana, A.D., Casal, A.J., Demareux, N., Vallotton, M.B., Capponi, A.M., Rossier, M.F., 1999. Angiotensin II negatively modulates L-type calcium channels through a pertussis toxin-sensitive G protein in adrenal glomerulosa cells. *J. Biol. Chem.* 274, 19943–19948.
797
798
799
800
801
802
803
804
805
806

- 807 Midzak, A., Rone, M., Aghazadeh, Y., Culty, M., Papadopoulos, V., 2011. Mitochondrial protein import and the genesis of steroidogenic mitochondria. *Mol. Cell Endocrinol.* 336, 70–79.
- 808
- 809
- 810 Miyoshi, H., Souza, S.C., Zhang, H.H., Strissel, K.J., Christoffolete, M.A., Kovsan, J., Rudich, A., Kraemer, F.B., Bianco, A.C., Obin, M.S., Greenberg, A.S., 2006. Perilipin promotes hormone-sensitive lipase-mediated adipocyte lipolysis via phosphorylation-dependent and -independent mechanisms. *J. Biol. Chem.* 281, 15837–15844.
- 811
- 812
- 813
- 814
- 815 Olichon, A., Baricault, L., Gas, N., Guillou, E., Valette, A., Belenguer, P., Lenaers, G., 2003. Loss of OPA1 perturbs the mitochondrial inner membrane structure and integrity, leading to cytochrome c release and apoptosis. *J. Biol. Chem.* 278, 7743–7746.
- 816
- 817
- 818
- 819 Pidoux, G., Witczak, O., Jarnaess, E., Myrvold, L., Urlaub, H., Stokka, A.J., Kuntziger, T., Tasken, K., 2011. Optic atrophy 1 is an A-kinase anchoring protein on lipid droplets that mediates adrenergic control of lipolysis. *EMBO J.* 30, 4371–4386.
- 820
- 821
- 822 Pralong, W.F., Hunyady, L., Várnai, P., Wollheim, C.B., Spät, A., 1992. Pyridine nucleotide redox state parallels production of aldosterone in potassium-stimulated adrenal glomerulosa cells. *Proc. Natl. Acad. Sci. USA* 89, 132–136.
- 823
- 824
- 825 Rizzuto, R., Simpson, A.W.M., Brini, M., Pozzan, T., 1992. Rapid changes of mitochondrial Ca^{2+} revealed by specifically targeted recombinant aequorin. *Nature* 358, 325–327.
- 826
- 827
- 828 Rodriguez, W.V., Thuahnai, S.T., Temel, R.E., Lund-Katz, S., Phillips, M.C., Williams, D.L., 1999. Mechanism of scavenger receptor class B type I-mediated selective uptake of cholesteryl esters from high density lipoprotein to adrenal cells. *J. Biol. Chem.* 274, 20344–20350.
- 829
- 830
- 831
- 832 Rone, M.B., Fan, J., Papadopoulos, V., 2009. Cholesterol transport in steroid biosynthesis: role of protein–protein interactions and implications in disease states. *Biochim. Biophys. Acta* 179, 646–658.
- 833
- 834
- 835 Satoh, M., Hamamoto, T., Seo, N., Kagawa, Y., Endo, H., 2003. Differential sublocalization of the dynamin-related protein OPA1 isoforms in mitochondria. *Biochem. Biophys. Res. Commun.* 300, 482–493.
- 836
- 837
- 838 Scorrano, L., Ashiya, M., Buttler, K., Weiler, S., Oakes, S.A., Mannella, C.A., Korsmeyer, S.J., 2002. A distinct pathway remodels mitochondrial cristae and mobilizes cytochrome c during apoptosis. *Dev. Cell* 2, 55–67.
- 839
- 840
- 841 Servetnick, D.A., Brasaemle, D.L., Gruia-Gray, J., Kimmel, A.R., Wolff, J., Londos, C., 1995. Perilipins are associated with cholesteryl ester droplets in steroidogenic adrenal cortical and Leydig cells. *J. Biol. Chem.* 270, 16970–16973.
- 842
- 843
- 844 Spät, A., Fülöp, L., Szanda, G., 2012. The role of mitochondrial Ca^{2+} and NAD(P)H in the control of aldosterone secretion. *Cell Calcium* 52, 64–72.
- 845
- 846 Spät, A., Hunyady, L., 2004. Control of aldosterone secretion: a model for convergence in cellular signaling pathways. *Physiol. Rev.* 84, 489–539.
- 847
- 848 Sperelakis, N., Schneider, J.A., 1976. A metabolic control mechanism for calcium ion influx that may protect the ventricular myocardial cell. *Am. J. Cardiol.* 37, 1079–1085.
- 849
- 850
- 851 Subramanian, V., Rothenberg, A., Gomez, C., Cohen, A.W., Garcia, A., Bhattacharyya, S., Shapiro, L., Dolios, G., Wang, R., Lisanti, M.P., Brasaemle, D.L., 2004. Perilipin A mediates the reversible binding of CGI-58 to lipid droplets in 3T3-L1 adipocytes. *J. Biol. Chem.* 279, 42062–42071.
- 852
- 853
- 854
- 855 Sukhorukov, V.M., Bereiter-Hahn, J., 2009. Anomalous diffusion induced by cristae geometry in the inner mitochondrial membrane. *PLoS One* 4, e4604.
- 856
- 857 Sztalryd, C., Xu, G., Dorward, H., Tansey, J.T., Contreras, J.A., Kimmel, A.R., Londos, C., 2003. Perilipin A is essential for the translocation of hormone-sensitive lipase during lipolytic activation. *J. Cell Biol.* 161, 1093–1103.
- 858
- 859 Tait, J.F., Tait, S.A.S., 1999. Role of cAMP in the effects of K^+ on the steroidogenesis of zona glomerulosa cells. *Clin. Exp. Pharmacol. Physiol.* 26, 947–955.
- 860
- 861
- 862 Tansey, J.T., Sztalryd, C., Gruia-Gray, J., Roush, D.L., Zee, J.V., Gavrilova, O., Reitman, M.L., Deng, C.X., Li, C., Kimmel, A.R., Londos, C., 2001. Perilipin ablation results in a lean mouse with aberrant adipocyte lipolysis, enhanced leptin production, and resistance to diet-induced obesity. *Proc. Natl. Acad. Sci. USA* 98, 6494–6499.
- 863
- 864
- 865 Tremblay, E., Payet, M.D., Gallo-Payet, N., 1991. Effects of ACTH and angiotensin II on cytosolic calcium in cultured adrenal glomerulosa cells. Role of cAMP production in the ACTH effect. *Cell Calcium* 12, 655–673.
- 866
- 867
- 868 Trzeciak, W.H., Boyd, G.S., 1974. Activation of cholesteryl esterase in bovine adrenal cortex. *Eur. J. Biochem.* 46, 201–207.
- 869
- 870
- 871 Vinson, G.P., Whitehouse, B., Hinson, J., 1992. *The Adrenal Cortex*. Prentice Hall, Englewood Cliffs, NJ, 07632.
- 872
- 873 Wasilewski, M., Semenzato, M., Rafelski, S.M., Robbins, J., Bakardjiev, A.I., Scorrano, L., 2012. Optic atrophy 1-dependent mitochondrial remodeling controls steroidogenesis in trophoblasts. *Curr. Biol.* 22, 1228–1234.
- 874
- 875
- 876 Wiederkehr, A., Szanda, G., Akhmedov, D., Matak, C., Heizmann, C.W., Schoonjans, K., Pozzan, T., Spät, A., Wollheim, C.B., 2011. Mitochondrial matrix calcium is an activating signal for hormone secretion. *Cell Metab.* 13, 601–611.
- 877
- 878
- 879 Wong, W., Scott, J.D., 2004. AKAP signalling complexes: focal points in space and time. *Nat. Rev. Mol. Cell Biol.* 5, 959–970.
- 880
- 881 Yamaguchi, T., Omatsu, N., Morimoto, E., Nakashima, H., Ueno, K., Tanaka, T., Satouchi, K., Hirose, F., Osumi, T., 2007. CGI-58 facilitates lipolysis on lipid droplets but is not involved in the vesiculation of lipid droplets caused by hormonal stimulation. *J. Lipid Res.* 48, 1078–1089.
- 882
- 883
- 884
- 885 Zhang, H.H., Souza, S.C., Muliro, K.V., Kraemer, F.B., Obin, M.S., Greenberg, A.S., 2003. Lipase-selective functional domains of perilipin A differentially regulate constitutive and protein kinase A-stimulated lipolysis. *J. Biol. Chem.* 278, 51535–51542.
- 886
- 887
- 888
- 889 Zimmermann, R., Strauss, J.G., Haemmerle, G., Schoiswohl, G., Birner-Gruenberger, R., Riederer, M., Lass, A., Neuberger, G., Eisenhaber, F., Hermetter, A., Zechner, R., 2004. Fat mobilization in adipose tissue is promoted by adipose triglyceride lipase. *Science* 306, 1383–1386.
- 890
- 891
- 892
- 893